TRI-PP-87-91
Dec 1987

Energy Response and Reaction Losses in Plastic Scintillators

Z. Papandreou, G.J. Lolos, G.M. Huber, J.C. Cormier, S.I.H. Naqvi, E.L. Mathie
Department of Physics, University of Regina, Regina, SK Canada S4S 0A2

D.F. Ottewell, P.L. Walden
TRIUMF, Vancouver, BC Canada V6T 2A3

G. Jones, R.P. Trelle
Department of Physics, University of British Columbia, Vancouver, BC Canada V6T 2A6

X. Aslanoglou[1]
Department of Physics, Florida State University, Tallahassee, FL 32306

S. Orfanakos
Department of Electronics, Educational Technological Institute, Athens, Hellas

Abstract

The energy dependence of the scintillation response (light output) of plastic scintillator BC400 has been investigated for protons in the energy region of 60 to 220 MeV. In this region the scintillation exhibits a linear response, as well as a noticable difference in the light output between stopping and passing-through (transmission) protons. A comparison between our results and theoretical calculations is presented. Losses due to edge effects have been separated from losses due to the bona-fide reaction of protons in the scintillator with the aid of Multi-Wire Proportional Chamber (MWPC) trajectory information. The number of events associated with reaction losses was found to range from 10% to 25% of the total number of events, depending on the incident proton kinetic energy.

[1]Present address: Department of Physics and Astronomy, Ohio University, Athens, OH 45701

1 Introduction

The response of plastic scintillator NE102 to protons and other charged particles has been reported elsewhere [1,2,3]. The type of plastic scintillator material used in this work was BC400, which has properties equivalent to NE102, and thus these results can be directly compared to the NE102 results cited above.

When linear response is important, it has been customary to use sodium iodide or cesium iodide crystals as total energy detectors for protons and heavier charged particles. In addition, these types of detectors can achieve an energy resolution of the order of 1%, making them desirable in nuclear structure studies where many closely lying states of a residual nucleus have to be resolved. However, these detectors have a long decay time rendering them unsuitable for use in experiments with counting rates above $\approx$ 10 kHz. The cost per unit volume is high, thus keeping the number of detectors used in a particular experiment low. This in turn implies a reduced solid angle and the sustained counting rate is degraded even further. Problems can also occur in attempting to match the timing of the slow NaI(Tl) signals with the fast signals of plastic scintillators when such a hybrid system is needed. A final drawback of these inorganic crystals is the large reaction tail associated with nuclear reactions in the crystal material [4].

On the other hand, plastic scintillators have some considerable advantages over NaI(Tl) for many types of experiments. Their response over a wide range of incident charged particle kinetic energies is non-linear, but when one is interested in a more restricted range they exhibit a linear behavior. Good energy resolution is always desirable, but not always critical. For reaction mechanism investigations on pion absorption experiments, for example, plastic scintillator detectors have a more than adequate energy resolution [5]. These counters, as is well known, can easily sustain counting rates of up to 4 MHz, and if their bases are transistorized, or if they have provision for an extra voltage boost on the last few stages of their dynode chains, they can achieve a 10 MHz counting rate without significant rate effects. Their cost per unit volume is considerably lower than that of NaI(Tl), thus allowing the use of a large number of plastic scintillator blocks during a single experiment while still keeping the total cost reasonable. One can effectively build a wall with such detectors, thus greatly increasing the solid angle and improving the counting rate of the apparatus. A final advantage of plastic scintillator detectors over NaI(Tl) counters is the fact that they have fewer reaction losses

than NaI(Tl). This was confirmed by the results of this work which agree with previously published data [6].

2 The Equipment

The detection apparatus has been described in detail elsewhere [5], however, a brief description will be given here.

The experimental apparatus consists of two arm-assemblies labelled "Arm-A" and "Arm-B". Each arm uses a $\Delta E - E$ counter arrangement. The ΔE counters are 0.5 cm thin and the E blocks on each arm have a total thickness of 30 cm. This is achieved in a single block on Arm-B and by stacking two 15 cm thick blocks one behind the other on Arm-A. With a total thickness of 30.5 cm and taking range straggling into consideration, protons of up to $\approx$ 220 MeV can be stopped within the active material. Two MWPCs, spaced 12.7 cm apart, are placed in front of the ΔE counters on each arm to provide particle location on the X and Y planes, with an intrinsic resolution of 1 mm along the scattering plane X and 2 mm in the Y plane. These MWPCs have an active area of 15×15 cm^2.

It is the front blocks on Arm-A that provide the information of interest on the response of the scintillators, while the Arm-B counters provide reaction tail information for a wider range of energies. The Arm-A blocks can stop protons of up to $\approx$ 140 MeV. Protons with higher energy than this pass through and stop in the blocks behind. We thus have a mixture of stopping and transmission spectra, each presenting a different light output.

The two arms are employed in a hardware coincidence together with a beam flux monitor, and the discriminator thresholds on the ΔE counters are set in such a way as to allow only a small number of pions to satisfy the coincidence, and thus provide a safety margin against gain or threshold shifts when looking at $\Delta E - E$ two dimensional plots.

3 Results and Discussion

Our data were obtained during a pion absorption experiment at the TRIUMF M11 medium energy pion channel. The detectors were calibrated via the $\pi^+ d \rightarrow pp$ reaction for various angle settings of

the two arms leading to different incident kinetic energies of the detected protons. For this purpose, pions of 100 and 165 MeV kinetic energies struck a deuterated polyethylene $(CD_2)^k$ target.

The performance of the apparatus [5] is characterized by a resolving power of the entire system of the order of 8.5 MeV, for a total kinetic energy of the two protons of 304 MeV. This translates to a 2.8% resolution in $\Delta E/E$ and 1.6% in $\Delta P/P$.

The light response of the front Arm-A E counters is shown in figure 1. The data has been normalized to the light output of a 100 MeV proton, and a least squares fit to this data is expressed by the linear equation y=ax+b, with a=86.08, b=15.02 (stopping), and a=73.86, b=7.78 (transmission). As can be seen, there is a large difference between the stopping and the transmission curves. This is believed to be a result of the quenching of the primary excitation by the high density of ionized and excited molecules [7]. In the last few MeV of a particle's energy before it stops, the ionization density is so high that the fluorescence of the scintillator saturates. The response of the detectors is clearly better for the transmission protons, since to produce the same amount of light as that produced by stopping protons a lower energy is required. In addition, since the relative light output of deuterons, tritons and other particles, with respect to protons, is known [1], our stopping and transmission curve fits can be used to predict the light output for any of these particles in plastic scintillator material.

For comparison of our results to theory, we have included the solid lines on figure 1 which were calculated using the method described in reference [1]. The equation used to calculate the light output was: $L = \int_{R_1}^{R_2} \log(1 + a \times dE/dr)dr$, where L is the light output, a=25.0 mg/MeV $\times$ cm^2 and $dE/dr = 16.94 \times r^{-0.448}$ MeV $\times$ cm^2/g for protons [1]. The length r is expressed in g/cm^2. The only difference between the transmission and stopping cases is in the lower limit of the integration. The upper integration limit R_2 is equal to the total range required to stop the proton in both stopping and transmission cases, whereas R_1 is equal to 0 in the stopping case and equal to $(R_2 - 15)$ cm in the transmission case. In the former case it is obvious that the integration takes place over the entire range of the proton since it eventually stops within the detector. In the latter case, however, no method to calculate the light output has been reported before and a method was devised and is explained below. For this case the integration takes place over 15 cm which represents the thickness of the front E counter which the protons transverse. It is not obvious, however, why these particular

limits are chosen, but the reasoning becomes clear when one relates the range to the proton energy that corresponds to it: R_2 corresponds to the energy the proton has when it strikes the front E counter and R_1 corresponds to the energy the proton has on exiting this counter. Hence to find the light output we, in effect, integrate the energy loss over the energy range that the proton has while transversing the front E counter. In figure 1 there appears to be a discrepancy between the data on the transmission protons and the calculated curve. Since the slopes of the calculated and fitted curves are almost identical, we believe that the difference between the two curves is due to the constant "a" used in the equation for calculating the light output. According to reference [1], a=25.0 mg/cm^2, and this value was obtained from fitting stopping proton data in the 1 to 14 MeV energy region. It appears that a different constant has to be used for the transmission case. Normalizing the theoretical curve to our data, in a first order approximation, leads to a constant a=27.0 mg/cm^2.

Reaction losses in various materials have been reported in the past [8,9,10]. When a proton passes through a material it can undergo nuclear interactions, and it is often important to know the number of these interactions, and to be able to separate them from losses due to other causes. For example, this knowledge is necessary when one wants to extract absolute cross sections. Losses can be caused by edge effects, in other words, a proton incident at a certain angle to the detector passes through the detector before depositing all of its energy. These are also known as purely geometrical losses.

The proton can also scatter elastically within the counter, and although elastic scattering is peaked forward and hence the proton normally stays within the confines of the sensitive volume, it sometimes scatters out of the detector and corrections have to be made. In addition, nuclear inelastic reactions are quite important. A proton interacts and produces deuterons, tritons and alpha particles, and although most of the energy of these particles is usually recovered, the energy deposited in the counter is less than that for the protons that stop in the detector without interacting. Finally, (p,γ) and (p,n) reactions also contribute to the losses. All of these processes remove protons from the full energy peak and produce a reaction tail from the lower energy side of the peak all the way down to the minimum energy threshold of the detector.

A detector system of the type used to collect the present data has never been reported for use in an experiment where high energy protons are stopped within the counters. It is known that the

probability of nuclear interactions occuring increases as the energy of the incident particle increases, and at very high energies the problem becomes serious enough that stopping detectors can not be employed. In the detected energy range of 60 to 220 MeV, however, the reaction losses are in fact a reasonable fraction of the total number of counts within a detector. Figure 2 shows an energy spectrum for a particular counter on Arm-B. The detected protons come from the $\pi^+(CD_2) \rightarrow ppX$ reaction and a ^{12}C subtraction has been performed, thus leaving only events from the $\pi^+ d \rightarrow pp$ reaction. The low energy tail, contained between arrows a and b, accounts for 35% of the total number of counts of this spectrum, for a full energy peak of 160 MeV protons. However, geometrical losses are included in this tail in addition to bona-fide reaction losses. To separate these two effects, software cuts are placed on the acceptance (opening) angle of the detector, which is defined by the MWPCs. The opening angle is actually defined by the X and Y dimensions of the counter at the calculated proton range in this counter. Figure 3 is a result of these cuts. In this histogram the tail has been reduced considerably, and now comprises 15% of the total counts in the spectrum. The percentage of the total number of counts in the tail, for various energies of the detected protons, is listed in table 1, and is plotted in figure 4. It should be noted that the errors in energy, listed in table 1, are due only to the kinematic spread in a 10 cm width of the detector; the uncertainty in the pion beam, or other errors, have not been folded in.

The performance of plastic scintillators with regard to reaction losses is indeed superior to that of sodium iodide crystals. This fact is not surprising considering that the reaction cross section for protons in NaI(Tl) is a factor of 8 higher than that in plastic [11].

Finally, when one examines a reaction on a nucleus larger than the deuteron, after eliminating the losses due to edge effects, it is possible to separate lower pulse height events arising from nuclear reactions from those due to "true" low energy particles by comparing the spatial energy loss distribution observed in the detector to that predicted from the range-energy relations for "true" particles [12]. An example of this can be seen in Figure 5 where the proton and deuteron bands are clearly separated. Pions can also be seen in the low energy region of this three-dimensional plot, and can be separated easily by applying appropriate software cuts.

Table 1: Reaction Losses in Plastic Scintillators for Protons

Reaction Losses (In percent of the total number of counts)			
Energy (MeV)	Energy Error (Kinematic Spread)	Losses (%)	Error in Losses (Statistical)
52	±4	10.6	±0.8
60	4	10.5	0.8
102	4	10.5	0.8
110	5	10.0	0.8
123	5	15.6	0.8
133	5	13.5	0.8
158	5	24.1	1.0
168	5	25.3	1.0
179	5	20.4	1.0
188	5	22.3	1.0

4 Summary

By using the fast scintillator spectrometer developed to investigate reactions of the type $\pi^{\pm}A \rightarrow ppX$, we have shown that the reaction losses in plastic scintillators are fewer than 30% of the total number of counts in the detected proton energy range of 60 to 220 MeV. We have also displayed the better light output response of these detectors to transmission protons than to that of stopping protons, and have derived an expression relating the proton light output to its deposited energy in plastic scintillator detectors.

Overall, for pion absorption experiments in which protons with kinetic energies below 300 MeV are detected, a MWPC – ΔE – E arrangement (with the E counters thick enough to stop these particles) has been found to be the most suitable and efficient detection apparatus because of its high counting rate capabilities, large solid angle and low reaction losses.

5 Acknowledgements

This project was supported in part by grants from the Natural Sciences and Engineering Research Council of Canada (NSERC). The generous assistance of Dr. E.W. Vogt, Director of TRIUMF, is also gratefully acknowledged.

References

[1] T.J. Gooding and H.G. Pugh, Nucl. Instr. Meth. **7** (1960)189.

[2] G.D. Badhwar et al., Nucl. Instr. Meth. **57** (1967)116.

[3] R.L. Craun and D.L. Smith, Nucl. Instr. Meth. **80** (1970)239.

[4] J.M. Cameron et al., Nucl. Instr. Meth. **143** (1977)399.

[5] Z. Papandreou et al., Nucl. Instr. Meth. (In press).

[6] D. Axen et al., Nucl. Instr. Meth. **118** (1974)435.

[7] J.B. Birks, The theory and practice of scintillation counting, (Macmillan, New York, 1964).

[8] M. Makino et al., Nucl. Instr. Meth. **80** (1970)299.

[9] D.F. Measday and C. Richard-Serre, Nucl. Instr. Meth. **76** (1969)45.

[10] P.U. Renberg et al., Nucl. Instr. Meth. **104** (1972)157.

[11] P.U. Renberg et al., Nucl. Phys. **A183** (1972)81.

[12] M Makino et al., Nucl. Instr. Meth. **81** (1970)125.

Figure Captions

Fig. 1: Deposited energies for protons are plotted versus light output for the 15 cm thick front counters of Arm-A. The dashed lines indicate least square fits for the stopping and transmission proton energy calibration cases, while the solid lines represent theoretical calculations via the method of reference [1].

Fig. 2: Proton energy spectrum of the $\pi^+ d \rightarrow pp$ reaction for an Arm-B counter with no cuts applied.

Fig. 3: Proton energy spectrum of the $\pi^+ d \rightarrow pp$ reaction for the same energy, angle and counter as that in Fig. 2, but now with the detector acceptance angle cuts applied.

Fig. 4: Energy dependence of proton reaction losses in plastic scintillators. The number of counts in the reaction tail of each spectrum, expressed as a percentage of the total number of counts, is plotted versus the $\pi^+ d \rightarrow pp$ full energy peak (in MeV) of the corresponding spectrum.

Fig. 5: Three-dimensional plot of ΔE versus E counters at $T_{\pi+} = 165$ MeV incident kinetic energy and $\theta_A = 90°$, $\theta_B = -63°$. The proton, deuteron and pion bands can be clearly seen.

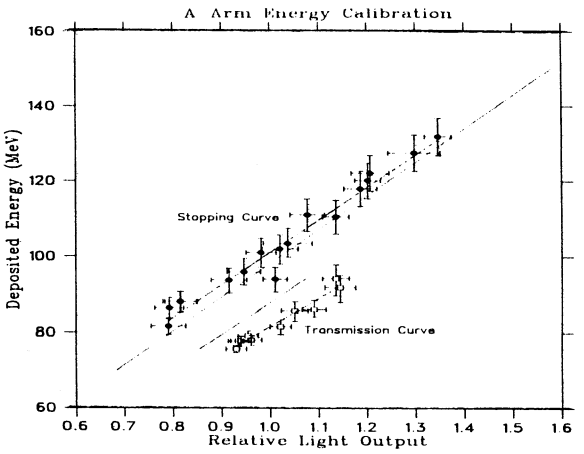

Fig. 1

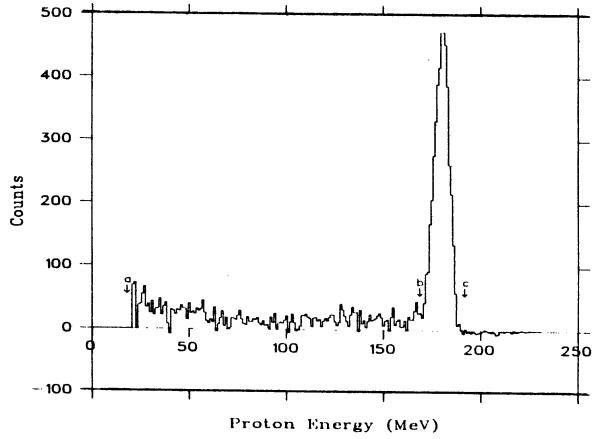

Fig. 2

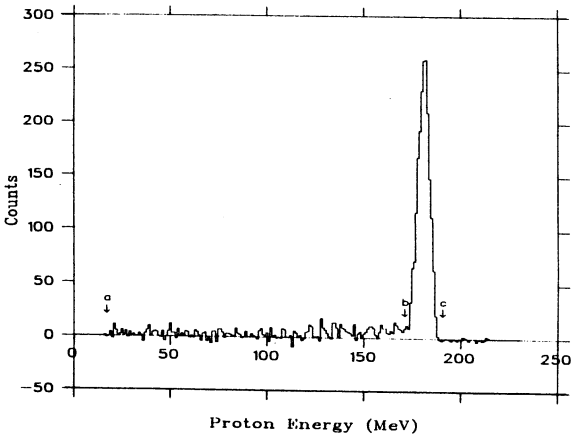

Fig. 3

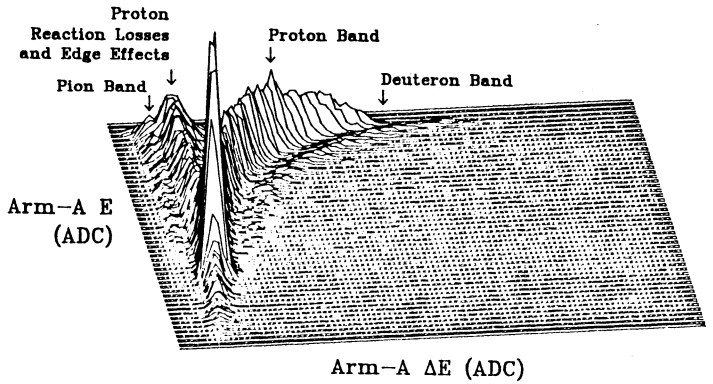

Fig. 5

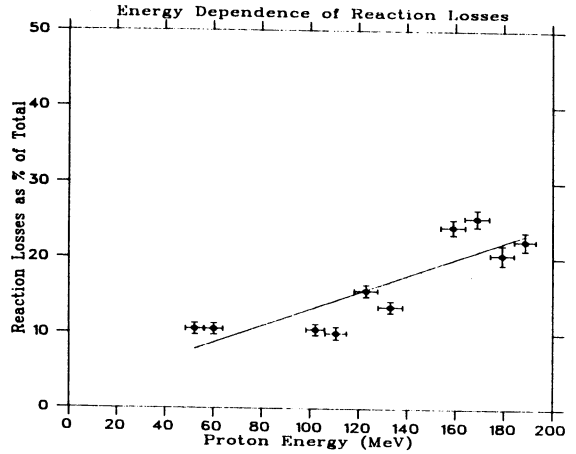

Fig. 4